Dendrochronologia 74 (2022) 125978

Contents lists available at ScienceDirect

Dendrochronologia

journal homepage: www.elsevier.com/locate/dendro

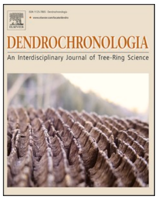

Temporal annotation of high-resolution intra-annual wood density information of *Eucalyptus urophylla* and its correlation with hydroclimatic conditions

Gleice Gomes Rodrigues [a,*,1], Martin Raden [b,1], Luciana Duque Silva [a], Hans-Peter Kahle [c]

[a] *Forest Science Department, "Luiz de Queiroz" College of Agriculture, University of São Paulo, Av Padua Dias 11, 13418-900 Piracicaba, Brazil*
[b] *Bioinformatics, University of Freiburg, Georges-Koehler-Allee 106, 79110 Freiburg, Germany*
[c] *Forest Growth and Dendroecology, University of Freiburg, Tennenbacher Str. 4, 79106 Freiburg, Germany*

ARTICLE INFO

Keywords:
Intra-annual wood density
Eucalyptus urophylla
Tropical dendroecology
Spatial alignment
Temporal annotation

ABSTRACT

Three different *Eucalyptus urophylla* clones grown under two different spacing regimes in an experimental site in the state of São Paulo, Brazil, were analyzed to test effects of clone identity, spacing, cambial age and hydroclimatic conditions on high-resolution intra-annual wood density profiles. Since distinct periodic tree-ring boundaries were not visible on the stem cross-sectional surfaces, finding an alternative method for synchronization of density profiles was crucial for the analysis. The challenge was to generate intra- and inter-tree synchronized density profiles that possess high amplitude variation and low phase variation. Thus, we developed a protocol and workflow of how such high-resolution density profiles can be spatially aligned and temporally annotated to enable correlation analyses between trees and with time series of environmental stimuli. Mean wood density was significantly different between clones, but not between the spacings. Wood density increased significantly with increasing cambial age and decreasing growth rate. Principal component analysis showed that the overall variability in the temporally annotated density profiles is dominated by a highly significant common signal. We found significant negative correlation values for precipitation, indicating that water supply is the main driver of stem growth at the site, and providing evidence for the correctness of the method. The developed workflow can easily be adjusted to the analysis of other intra-annual tree-ring features like anatomical xylem cell traits or isotopic signals in the wood. It has a large potential to be used as a general guideline for the synchronization of intra-annual tree-ring traits, especially when distinct tree-ring boundaries are missing, as it is often the case under tropical climatic conditions. The workflow supports the development of spatially aligned and temporally annotated chronologies under non-annual growth rhythms.

1. Introduction

The forest plantation area has been rapidly increasing in the world, especially in the tropical and sub-tropical regions of South America, South East Asia, and Africa (Brown et al., 1997; FAO, 2014). *Eucalyptus* species and their interspecific hybrids stand out with extensive cultivated areas, mainly because they present high average productivity (41 m^3 $ha^{-1}.yr^{-1}$; FAO, 2014) and are highly adaptable to environmental conditions (Myburg et al., 2014).

Although several studies on coniferous species have examined the effects of climatic variables on the formation of wood growth rings (Allen et al., 2012; Drew et al., 2012), most *Eucalyptus* species lack basic information about their dendroclimatological potential. This is due to the fact that, under tropical and sub-tropical conditions, most species of the genus do not show distinct annual growth rings that can be dated exactly in its calendar year of formation (Argent et al., 2004; Brookhouse, 2006). This is the case for *Eucalyptus urophylla*, i.e. that so far, none of the published works related the climate to the width of the rings or the gravimetric density of the wood.

In dendro-climatological studies, climatic factors, such as monthly precipitation sums and average air temperature, are associated with growth traits such as tree-ring parameters. Interestingly, tree-ring wood density often yields closer correlations with climate data than tree-ring width (Polge, 1970; D'Arrigo et al., 1992; Briffa et al., 2002; Drew et al.,

---

* Corresponding author.
E-mail address: gleice.florestal@gmail.com (G.G. Rodrigues).

[1] GGR and MR should be considered joint first author

https://doi.org/10.1016/j.dendro.2022.125978
Received 16 January 2022; Received in revised form 18 May 2022; Accepted 30 May 2022

2012). One of the most recent technologies that has been used to determine the variation of intra-annual density is the high-frequency densitometry method, developed by Schinker et al. (2003). In addition to being highly accurate, measurements with high-frequency densitometry are very efficient and processing time is relatively short (Wassenberg et al., 2014). Some studies have already used high resolution intra-annual wood density data to correlate them with climate data (i.e. Drew et al., 2011; Oliveira et al., 2011; Koprowski and Duncker, 2012; Franceschini et al., 2013; George et al., 2019; Mayer et al., 2020).

In general, in tropical regions, the environmental factors that most influence the cambial activity of trees and, therefore, variations in wood density profiles, are precipitation and water availability (Cosgrove, 2016; Wils et al., 2009). Historically, the southeastern region of Brazil has a well-defined annual precipitation cycle, with maximum rainfall in the months from December to February (summer) and minimum values during the period June-August (winter) (IBGE, 1972). However, in 2014, due to the much lower rainfall than the historical average, the region faced one of its worst droughts ever recorded, mainly affecting the state of São Paulo. Therefore, it is expected that, since periods of climatic adversity have an impact on the development of trees as evidenced by their radial growth (Schweingruber, 1982), high resolution measurements of density will provide useful information for assessing intra-annual growth rates and for the reconstruction of weather patterns and climate based on tree-rings (Worbes, 2002).

Considering the importance of wood density as a key trait to predict wood quality for industrial uses, and the role of weather and climate as important determinants of tree growth, the present study aimed to develop chronologies of high resolution intra-annual tree-ring density for clonal plantations of *Eucalyptus urophylla* subject to two planting spacings in southeastern Brazil and assess their synchronicity and sensitivity to climatic variables.

Annual tree-ring boundaries were absent in our *Eucalyptus urophylla* sample material. However, on the cross-sections we could identify radial variations in visible wood properties due to concentric variations in cell geometry, cell type arrangement and wood color, that seemed to be aligned within trees and synchronized between nearby trees. Since we knew precisely the age of the trees, we could verify by counting that these concentric bands or "growth-rings" (IAWA, 1964) were not of annual nature. For the purpose of this study, we developed and applied a method to align such growth ring patterns of seemingly variable but unknown rhythm within and between trees and to map and annotate these patterns on a time axis. We used high resolution cross-sectional micro-density data of wood together with wood anatomical information derived from the analysis of stem cross-sections as growth parameters, and correlation with time series of environmental stimuli to validate the method (Stahle, 1999).

We define this registration problem as the search for a set of data processing steps to generate intra- and inter-tree synchronized density profiles that possess high amplitude variation, i.e. amplified density signal strength, and low phase variation, i.e. minimized noise due to temporally varying differences in growth speed among and between individual trees.

2. Material and methods

2.1. Study site and climate data

Thirty-six clonal *Eucalyptus urophylla* trees were monitored in the central-southern region of the state of São Paulo at the Experimental Station of Forest Sciences of Itatinga (University of São Paulo - USP) (850 m a.s.l., 23°10' S and 48°40' W). According to the Köppen classification, the climate of the region is defined as Cfa: humid temperate climate with hot summer. The soils were very deep Ferralsols (>15 m) on Cretaceous sandstone, Marília formation, Bauru group, with a clay content ranging from 14% in the A1 horizon to 23% in deep soil layers (Laclau et al., 2010; Christina et al., 2011; Battie-Laclau et al., 2014). Chemical soil analysis revealed that the levels of Phosphorus (P), Magnesium (Mg), Aluminum (Al) and Cation Exchange Capacity (CEC) decreased with increasing depth. The stocks of Calcium (Ca) and Potassium (K) were at very low levels as well as the base saturation (<6%). The meteorological data of mean temperature (ºC), precipitation (mm), relative humidity (%), wind speed ($m.s^{-1}$) and solar radiation ($MJ.m^{-2}$) were obtained in intervals of 30 min, using an automatic measurement station present in the headquarters of the experimental station. The climatic water balance was estimated through the reference evapotranspiration (ETo) adopting the FAO-56 Penman-Monteith (FAO-56 PM) method (Allen et al., 1998). The monthly values of mean temperature, precipitation, and climatic water balance are shown in Fig. 1a and b. The average annual rainfall sum and average annual temperature from January 2012 to December 2019 was 1.698 mm and 19.6 °C respectively. During the measurement period the data show a distinct temperature seasonality with a low temperature season regularly occurring from June to September (winter). Seasonality in precipitation with peaks during December to February (summer) is also visible, however, inter-annual variation in precipitation sums is also large, and much larger than for temperature.

2.2. Experimental design

The experiment was set up in January 2012 on a site that was previously a commercial area planted with *Eucalyptus sp.* without specific treatment. The experimental design was a randomized block design, with a 3 × 2 factorial scheme, consisting in the planting of three commercial *Eucalyptus urophylla* clones (AEC 144, AEC 224 and COP 1404) at two spacings (3 m x 2 m, or 3 m x 4 m), with 3 replicates (see Table 1). Square plots of 25 plants (5 rows x 5 plants) were installed. Considering buffer zones between treatment plots, the 9 central plants per replicate were considered for sampling for the analysis of tree growth.

The clones were selected according to their productivity and tolerance to water deficit conditions, based on data from the companies that use these materials in their commercial plantations. In detail, these are clones AEC 144 and AEC 224 with high and medium-high tolerance to water deficit conditions, respectively, and clone COP 1404 with low-medium tolerance to water deficit and high temperature conditions. The planting site was prepared by applying the minimum tillage with subsoiling treatment between the planting rows of the previous rotation. This procedure mobilizes the soil by to breaking up compacted or dense layers until 0,40 m of soil depth. Ants control was performed systematically using sulfluramid-based formicide baits and chemical weed control was performed until the canopy closure (1 year). Plants received base fertilization to improve soil nutrient supply and supplemental fertilization at the age of 8 months (for details on fertilization treatments see Rodrigues et al., 2021).

2.3. Sample preparation and high-frequency (HF) densitometric measurements

To determine the cross-sectional density profiles, 6 of the 9 central trees per clone-spacing combination were selected according to the diameter class, and felled in June 2019 at an age of 7 years. From each sample tree, disc samples at 1.3 m stem height (breast height) were collected.

The stem-discs were air-dried for 1–2 months, and the upper cross-sectional surface of each disk was smoothed using an ultra-precise diamond fly cutter (Spiecker et al., 2000). High-frequency (HF) densitometric measurements were conducted with a prototype densitometer located at the Chair of Forest Growth and Dendroecology, University of Freiburg. All measurements were conducted with the same HF-probe with maximum measurement resolution in radial direction of 110 μm and tangential width of the measurement slit of 1.757 μm. Measurements were taken every 28 μm. On each disc, four evenly spaced radii

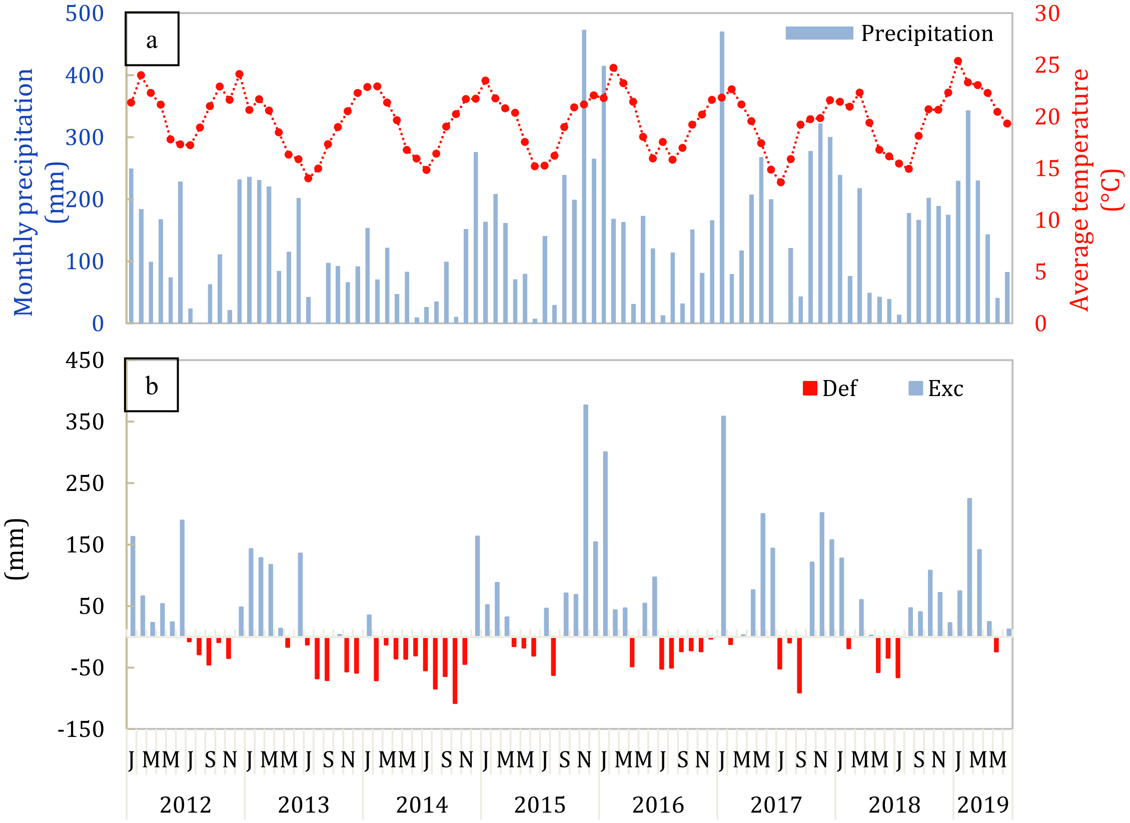

Fig. 1. a) Monthly rainfall (mm) and monthly mean air temperature (°C) recorded at the study site from January 2012 to June 2019. b) Climatic water balance (water deficit = Def; water excess = Exc) calculated using Penman-Monteith method (FAO-56 PM).

Table 1
Characterization of the experiment. DBH: Diameter at breast height (mean, and values ranges corresponding to minimum and maximum.

Spacing	Clone	Number of trees	DBH (cm)
3 m x 2 m	AEC 144	6	15.0 / 12.4–17.8
	AEC 224	6	16.7 / 15.0–20.3
	COP 1404	6	11.7 / 8.4–14.6
3 m x 4 m	AEC 144	6	18.8 / 13.3–22.6
	AEC 224	6	18.4 / 13.5–20.1
	COP 1404	6	17.3 / 13.5–18.6

were scanned with the HF-probe, from pith to bark. The measurement data of the HF-densitometric analysis was rescaled to units of gravimetric density (Wassenberg et al., 2014).

2.4. Data processing

In the following we introduce the protocol and workflow of how such high-resolution density profiles of *Eucalyptus urophylla* can be mapped on a time axis to enable correlation analyses between different trees and with time series of environmental stimuli. The multi-step approach is summarized in Fig. 2 and detailed below. For clarity, key terms are explained in Table 2.

2.4.1. Steps 1 and 2 - consensus density profile per tree

To reduce the noise in the density data from the individual HF-measurement series and to obtain a single aggregated density profile per sample tree, the four-measurement series per tree were aligned in a semi-automated process similar to (Bender et al., 2012). In eucalypt species, growth-ring boundaries are often indistinct (Brookhouse, 2006), making it necessary to adopt appropriate techniques that allow detecting subtle changes in wood structure that are aligned within (and later synchronized between) individual trees. Radial variations in wood anatomical properties such as tracheid, fiber or vessel characteristics are ultimately driven by temporal changes in cambial activity and subsequent xylogenesis processes (Sette et al., 2016). Cambial activity in turn is synchronized between nearby trees by the temporal course of environmental stimuli (Tomazello Filho et al., 2004). Thus, in order to support the alignment of multiple density measurement series obtained within a sample tree, microscopic images of the cross-sectional wood anatomy along the same measurement radii were used. Sequences of anatomical marks as changes in fiber geometry or in the color, shared among several radii per sample tree were visually identified on the microscopic images, which is illustrated in Fig. 3. Since many of the identified distinct anatomical marks had correspondent marks in the density measurement series (Roque and Tomazello Filho, 2007; Oliveira et al., 2011; Melo et al., 2016), the positions of the anatomical marks were transferred and mapped to the density measurement series. Subsequently, the density series between mapped marks were synchronized using the MICA curve alignment software (Mann et al., 2018). From the resulting set of aligned density profiles, a consensus profile was obtained per tree, representing the mean profile at respective radial positions (spatial alignment, intra-tree consensus profile).

In detail, each anatomic mark was relocated to the mean radial position of this mark within all radial measures and intermediate data was linearly interpolated. That way, all measurement series were normalized to their average length and segmented into equally long intervals between the marks. To amplify signal strength, LOESS smoothing of the raw data with a bandwidth of 20 data points was done. Intervals from respective segments were subsequently aligned using MICA (setting both max. X shift and min. interval length to 20 data points and max. warping factor to 1.5).

MICA optimizes the mapping of subcurves with similar slopes. Slope values were based on normalized density data (z-score). The MICA-

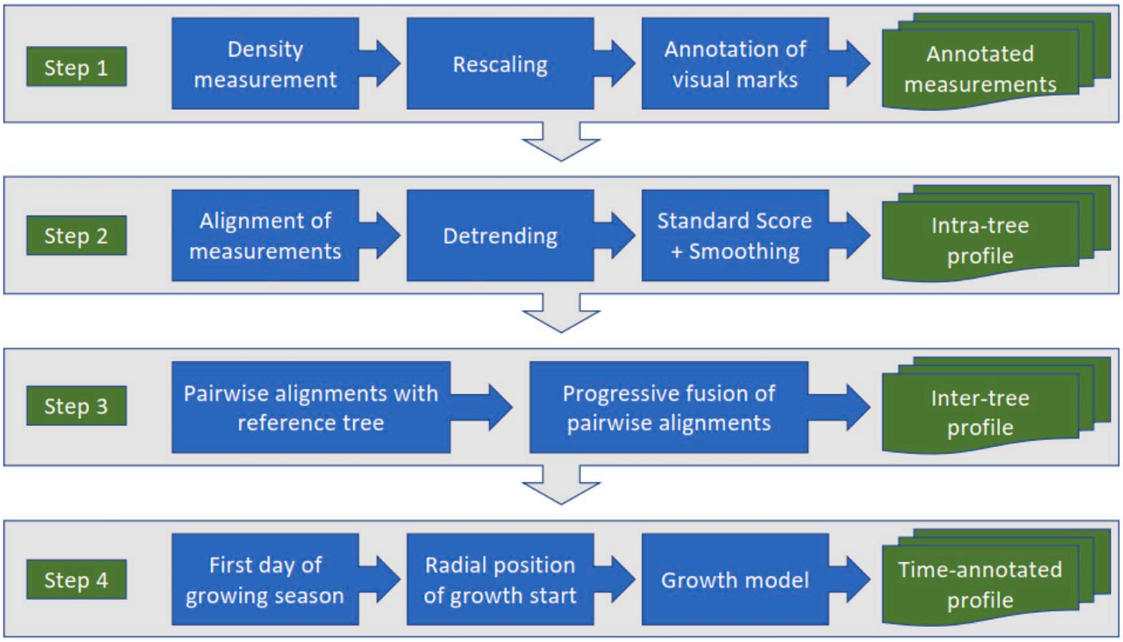

Fig. 2. Flowchart of data processing steps. (Step 1) Per sample tree: after surface preparation of stem cross-sections, HF-density measurements were performed in four radial directions. After rescaling them to gravimetric density, multiple pronounced visual anatomical marks were annotated in each radial density measurement series based on high-resolution images. (Step 2) The visual marks allow for an automated alignment of the measurement series per tree. The resulting averaged intra-tree consensus profile was detrended, standardized (Z-score normalization) and smoothed (LOESS). (Step 3) Each intra-tree consensus profile was manually aligned with a reference tree density profile. This enables a reference-guided generation of multi-tree alignments from which representative inter-tree density profiles are derived for all trees or subsets. (Step 4) By estimating radial positions marking the start of growing seasons and respective days of each year, a non-linear growth model was derived. This was subsequently used to warp the density profiles onto a time axis (temporal annotation).

Table 2
Summary of the key terms and definitions needed to present the workflow to temporally annotate high-resolution density data.

Term	Definition
Density measurement	Single density value
Density measurement series	Sequence of density values along a measurement line/radius
Spatial alignment	Warping of the spatial position information of two density measurement series to map respective/similar subsequences onto each other
Density profile	Averaged (consensus) density series derived from spatially aligned measurement series
Intra-tree density profile	Density profile derived from all density measurements of one tree
Inter-tree density profile	Density profile derived from aligning the density profiles of a group of trees
Temporally annotated density profile	Density information mapped onto a time axis

optimized warping of the intervals was then used to get the final alignment of all intervals and segments per tree. From this, a single aggregated consensus density profile per tree was derived as the average value at respective radial positions.

Finally, each tree's consensus profile was detrended, since all trees showed increasing wood density with increasing age or dimension (see Fig. S1). To this end, a trend was fitted using the asymmetric least square method (Eilers, 2004) implemented in the *baseline* package (v1.3–1) from R. Subsequently, the consensus profile was divided by the respective trend values (to detrend the data) and standardized via z-transformation. This procedure amplified low density fluctuations, facilitating the subsequent multi-tree alignment.

2.4.2. Step 3 - multi-tree alignment based on pairwise mappings

To enable a comparison of respective density patterns between trees and to allow for the aggregation of growth data of subsets of trees, a multi-tree alignment of the consensus data was done. To this end, first, pairwise alignments of each tree with a predefined reference tree (W38: AEC 144, 3 m x 4 m) were manually generated via visual inspection and alignment using a dedicated interactive R implementation. A depiction of a final pairwise alignment is given in Fig. 4. While any tree could have been used as reference to "link" the alignments, W38 was selected since it showed on average the lowest distance to unaligned consensi. Similar to the intra-tree alignment based on visual marks, the mapped positions segment the density profiles. Due to the high number of manually aligned positions, segments are directly warped via linear interpolation instead of further aligning them using MICA. As a result, we obtained a mapping of all spatial positions of the reference tree onto the aligned tree and vice versa.

This resulting pairwise mapping information with respect to the reference tree enables a progressive generation of the multi-tree alignment. To this end, trees are iteratively added to a growing multi-tree alignment. In contrast to the pairwise alignment, the computation of new radial positions has to be weighted. That is if the current alignment already includes n trees (including the reference), the new (aligned) position of the reference's coordinate i (which represents all coordinates of already aligned trees) and the coordinate j of the tree to be added is $(n * i + j)/(n + 1)$. Eventually, we derive a final multi-tree alignment of all trees, from which we can derive a single averaged consensus density profile as an aggregate of all sample trees.

2.4.3. Step 4 - modelling annual growth for temporal annotation

Most likely the speed of radial growth of the Eucalyptus sample trees is not constant, i.e., non-linearly related to time. Thus, there is the need to map the radial axis of the density profiles onto a time axis before correlating density data between different trees or with time series data of environmental stimuli.

Given for each year from 2012 to 2018 a specific day that marks the beginning of the growing season, we can fit an annual growth model for a given density curve as follows. Respective days were selected based on

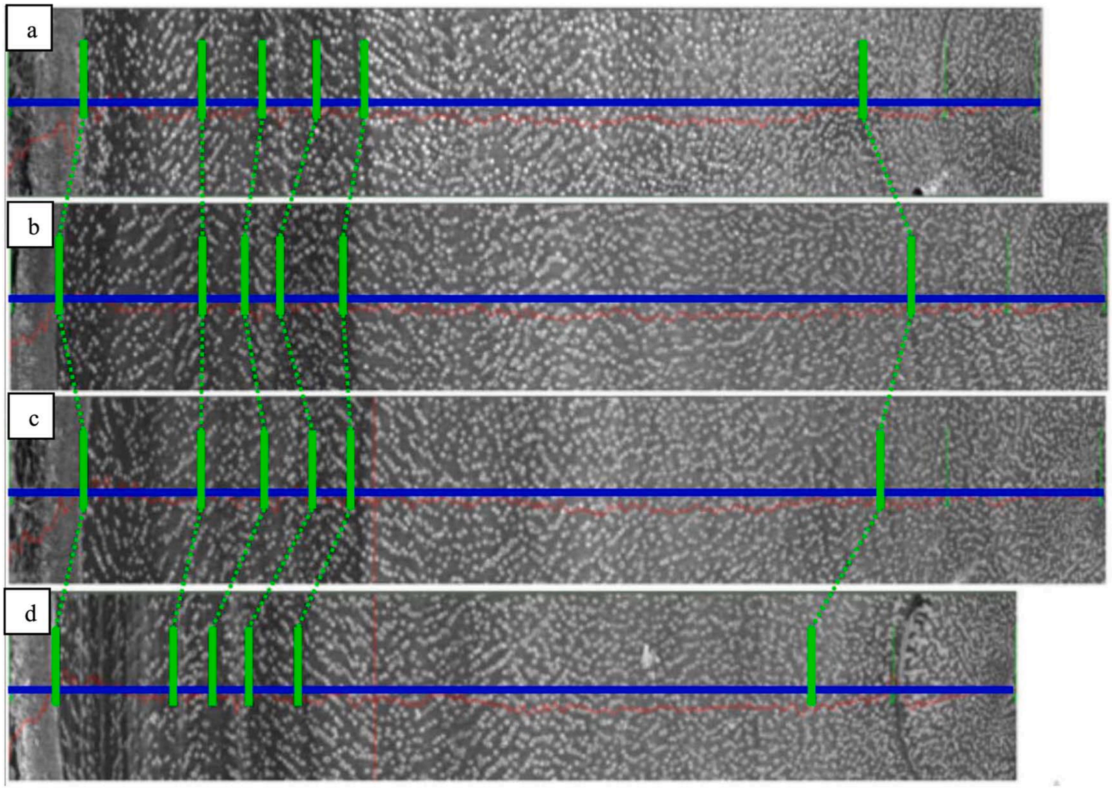

Fig. 3. Depiction of high-resolution images (gray scaled) of the four radial directions (a-d, pith on the right) along which density measurement series were taken (blue lines). Green solid bars indicate manually annotated wood anatomical marks that are common among all four radii and thus are considered to be synchronous (dotted green lines).

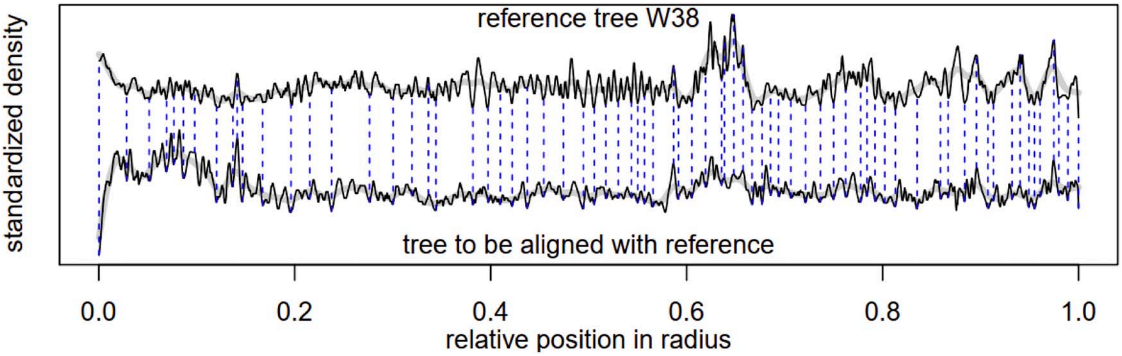

Fig. 4. Visualization of the pairwise alignment of a tree's consensus density profile (bottom, black) with the reference tree W38 (top, black). The trends are highlighted by respective thick gray lines. Manually aligned positions are highlighted by vertical dashed blue lines, i.e., they have been shifted to their respective average positions.

cumulative two-week precipitation data, i.e. for each day of the year the precipitation of the preceding 14 days was summed. As the start of the growing season, we picked the last day of the year after which a smoothing spline of the cumulative precipitation was above 30 mm for the rest of the year. This resulted in the days 2012–12–04, 2013–11–23, 2014–11–04, 2015–08–27, 2016–10–07, 2017–09–27, 2018–09–07.

Next, we identified respective radial positions within density profiles. For this, we manually picked the last dominant maximum of a distinct bell-shaped peak of the density curve. This is done under the assumption that (a) the wood built at the start of the growing season will be of lower density, which (b) manifests itself as a sharp density drop in radial (growth) direction. Ultimately, only for the years 2014–2018 such a distinct maximum could be identified based on visual inspection.

Given the day of the beginning of the growing season and given the radial position of the distinct density maximum, we fitted an interpolating spline (radial position vs. day) as the final model for temporal annotation. That way, for each day the respective radial position and thus the density data is derived via linear interpolation. Since the later years in the observation period 2012–2018 correspond to much shorter radial ranges, i.e. smaller annual growth rates, individual years' density data shows strong variations in detail, which is depicted in Fig. 5. This problem is amended using a final smoothing spline (spar = 0.2) of the temporally annotated density profile. Finally, this provides us with high resolution density information on a time axis.

2.5. *Statistical analyses*

The data processing and analyses were carried out with the R software (R Core Team, 2020). The basic assumptions for analysis of variance (ANOVA) were evaluated at a significance level of 5%, normality

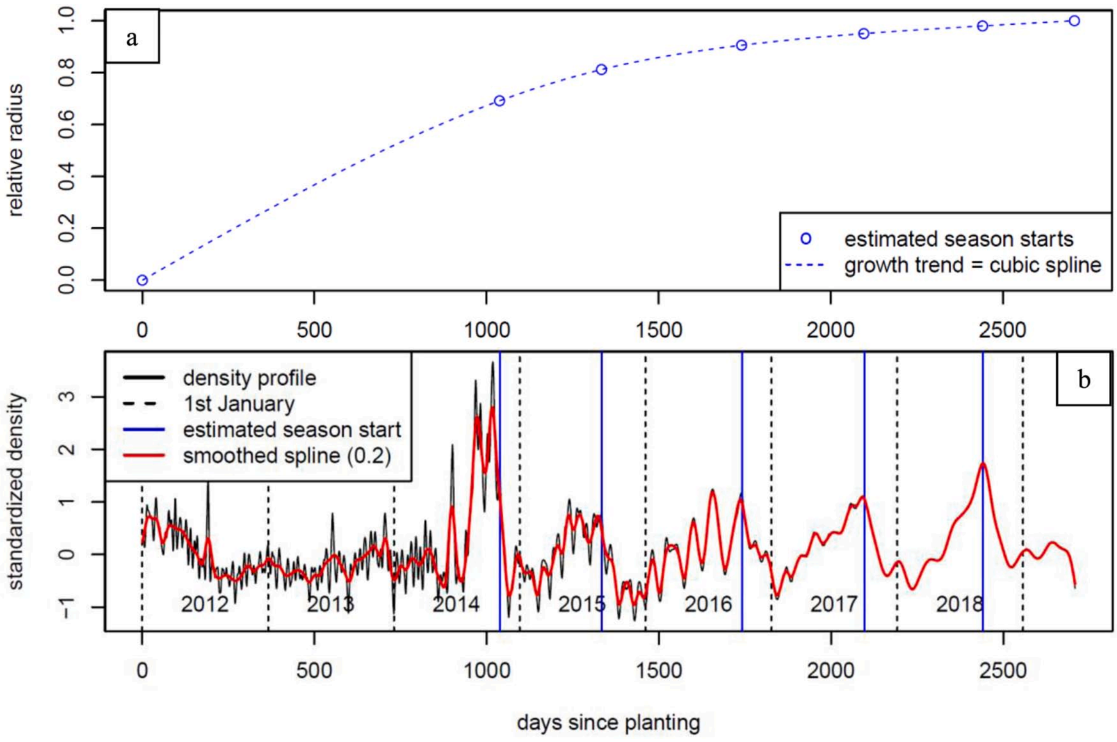

Fig. 5. (a) Growth model for all trees of this study based on mappings of annual starts of growing seasons to radial positions. (b) The model was used to replace radial positions of the inter-tree density profile with respective time information, which results in the temporally annotated density profile representing all trees.

test and homogeneity of variances.

Significance of correlation values for time series comparisons was assessed based on the effective sample size. Following Dawdy and Matalas (1964), we calculated the effective sample size N' of two time series X and Y, both of length N, by.

$$N' = N * (1 - r1(X)*r1(Y)) / (1 + r1(X)*r1(Y))$$

where r1(.) provides the first-order autocorrelation coefficient (Pearson correlation coefficient of lag-1 data, i.e. intervals [1,N-1] with [2,N]). The effective sample size N' is used to assess the significance of the correlation value.

Principal component analysis (PCA) was used to analyze the multivariate matrix of temporally annotated density profiles of different subsets of trees with the aim to assess the strength of the common signal in the density profiles and to test the significance of genetic material (clone) and planting setup (spacing) on the wood density profiles.

3. Results

3.1. Wood density and stem growth rate

The mean gravimetric wood density varied from 0.47 to 0.59 g cm^{-3} among the clone-spacing combinations. Although no significant differences were observed in the mean wood density between the evaluated spacings, the clones differed from each other, with the highest average observed in clone COP 1404, in both spacings, with 0.57 g cm^{-3} (3 m x 2 m) and 0.59 g cm^{-3} (3 m x 4 m) (see Table 3).

Clone COP 1404 had the highest mean wood density and lowest mean DBH (see Table 1), and consequently the lowest mean stem diameter growth rate when compared with the other genetic material evaluated (Fig. 6). Our research material does not show a statistically significant relationship between mean wood density (g cm^3) and mean monthly stem diameter growth rate (cm $month^{-1}$) for any of the clones (Fig. 6).

Table 3
Gravimetric wood density of the sample trees (mean (standard deviation in brackets), minimum, and maximum). Different lowercase letters indicate significant differences within a spacing ($p = 0.05$). Different uppercase letters indicate significant differences between the two spacings for a given clone.

Spacing	Clone	Density (g cm^{-3})		
		Mean	Minimum	Maximum
3 m x 2 m	AEC 144	0.50 (0.05) b A	0.44	0.57
	AEC 224	0.49 (0.04) b A	0.45	0.54
	COP 1404	0.57 (0.02) a A	0.55	0.60
3 m x 4 m	AEC 144	0.48 (0.05) b A	0.40	0.56
	AEC 224	0.47 (0.03) b A	0.43	0.50
	COP 1404	0.59 (0.02) a A	0.56	0.62

3.2. Temporal annotation of high-resolution density data

For all 36 trees, four high-resolution density measurements were aligned, averaged, standardized and smoothed for each tree. As a result, a single aggregated density profile was derived for each tree.

Within the period of growth (2012–2018), the year 2014 is known for its extreme drought (Fig. 1). When investigating the densitometric data, we find at about 0.6–0.7 relative radial position a distinct density peak (Fig. S2) that is common to all trees. The same peak is followed by four unique but less spiked peak shapes at decreasing widths. We thus conclude that the prominent peak relates to the drought of 2014 and the subsequent peaks correspond to the summer seasons of 2015–2018.

For different subsets of trees, respective multi-tree alignments were computed. Namely one alignment covering all trees (Table 1) and one for each subgroup based on clones (AEC 144, AEC 224, COP 1404) and spacing (3 m x 2 m and 3 m x 4 m) as well as their combinations.

For each consensus density profile of a multi-tree alignment, individual approximate radial positions corresponding to the start of annual growth seasons were selected. These were used to derive subgroup-specific annual growth models that were applied to temporally annotate the density profiles for each subset of trees.

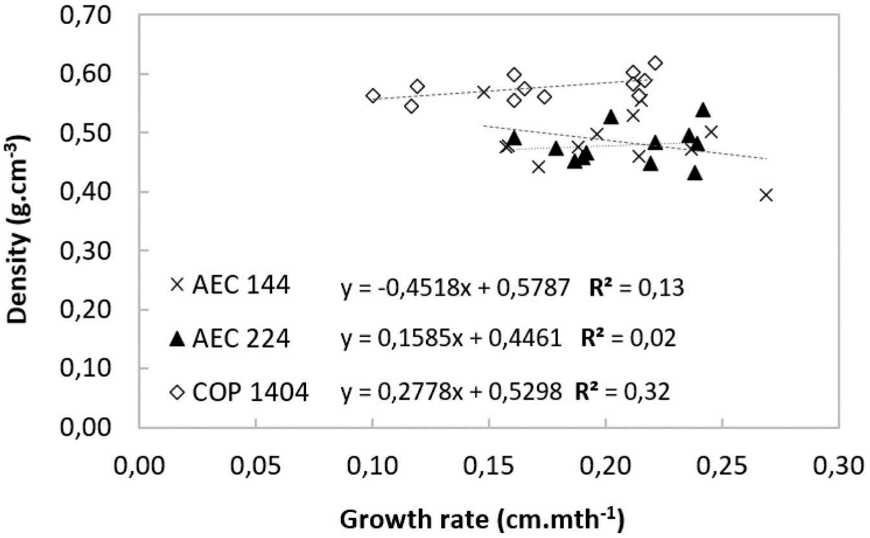

Fig. 6. Mean gravimetric wood density (g cm^{-3}) versus mean growth rate (cm month^{-1}) with the equation by clone and the determination coefficient (R^2). Dotted lines represent linear trendlines fitted by clone.

3.3. Comparison of density profiles

Temporal annotation is the premise for a meaningful quantitative intercomparison of density profiles, since it removes the individual-specific growth dynamics that distort the synchronicity of the density profiles when arranged on a spatial, i.e. radial, axis. We found a significant relation between high-resolution wood density and daily relative growth rate (negative, Fig. S4a) as well as with cambial age (positive, Fig. S4b). Since both factors are confounded, it is, based on the given material, not possible to clearly discriminate the effects of these two possibly causal relations. For further analyses we focus on the period 2015–2018, excluding juvenile wood as well as the year 2014 which was strongly affected by the long lasting and intensive drought during 2013/2014 (Fig. 1) (final number of data points: 1.460; 1 data point per day).

Fig. 7 summarizes the results of the principal component analysis (PCA) in terms of factor loadings of the first three principal components (PC). PCA of the combined grouping by clones and spacings ($n = 3 \times 2$) shows, that the overall variability in the temporally annotated density profiles is dominated by a highly significant common signal, PC1, explaining 77.2% of the overall variance (Fig. 7). Grouping by clones ($n = 3$) results in 85.8%, and grouping by spacing ($n = 2$) in 93.2% of variance explained by PC1 (not shown). The other PCs, and hence the effects of clone and spacing, were insignificant (eigenvalue < 1).

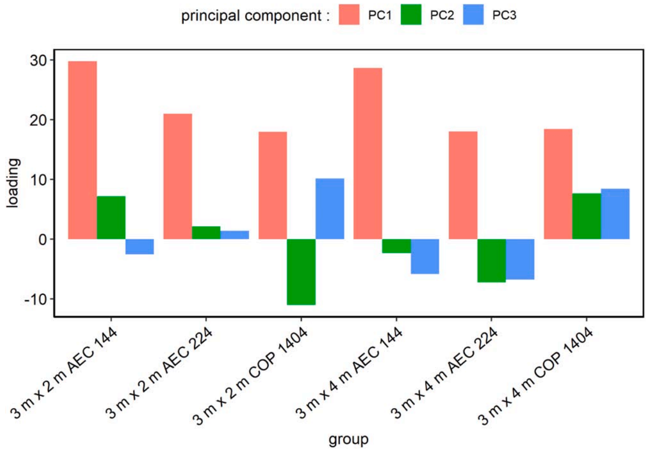

Fig. 7. Factor loadings of the first three principal components (PC1, …, PC3, color coded) shared among clone-spacing grouping (n = 3 clones x 2 spacings) of temporally annotated density profiles (period: 2015–2018, number of data points (days): 1.460).

3.4. Relation of density profiles and environmental factors

We correlated the temporally annotated density profiles with time series of environmental factors for the period 2015–2018 to study the impact of the latter on the tested clones and treatments. In detail, we compared the density profiles with time series of precipitation and water balance. Since the growth response does not materialize instantaneously but with some time delay, we compared the density profiles with lagged 14-day cumulative values of precipitation and climatic water balance. Equivalent to the density data, time series of the environmental factors have been smoothed (spline with spar = 0.2, see Fig. S3 for an example). Fig. 8 summarizes results of the correlation analyses for various subsets of trees.

We observe similar negative correlation values for precipitation and climatic water balance ranging from − 0.2 to − 0.36, while precipitation showing the stronger correlation (higher absolute values). Furthermore, only precipitation correlations yield p-values below 0.1 (color coding and star-annotation in Fig. 8). Strongest and most significant correlations (p-value < 0.05) are observed for the density profiles of all trees and of all trees in spacing 3 m x 4 m. Among the clones, AEC 144 shows the strongest correlations (p-value < 0.1), followed by COP 1404 and AEC 224. COP 1404 correlates highest (p-value < 0.1) for the 3 m x 4 m treatment, while the 3 m x 2 m spacing shows higher correlation for the other clones when compared to the wider spacings.

4. Discussion

4.1. Effects of clone-identity and spacing on wood density

In one of the first systematic studies on variations in wood anatomy within Eucalyptus species, Wilkes (1988) found that Eucalyptus species are characterized by substantial genetically predetermined within and between-tree variations in wood anatomical features. Wilkes stated that the effect of genotype outweighs by large that of growing conditions, and that observed differences in wood quality between plantation stands and old growth forests are mainly due to the greater proportion of juvenile wood in small, rapidly grown sterns.

In their review study on the effects of silvicultural treatments on wood properties of Eucalyptus species Gonçalves et al. (2004)

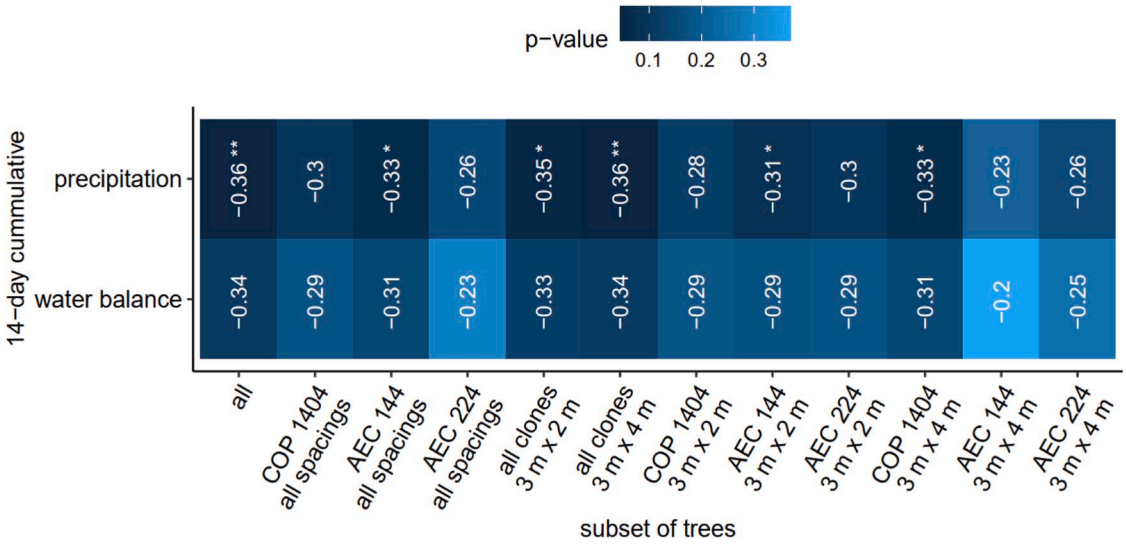

Fig. 8. Pearson correlation values for temporally annotated inter-tree density profiles of various subsets of trees (x-axis) versus two environmental signals, namely 14-day cumulative precipitation and climatic water balance. Correlation was computed for the time frame 2015–2018. The color indicates the significance of the correlation values in terms of p-values. '* ' or '* *' highlight p-values below 0.1 or 0.05, respectively.

concluded, that there is no general correlation between growth rate and wood basic density. The finding that wood density in Eucalyptus species is primarily under genetic control, and less affected by environmental factors is corroborated also by more recent studies (Frederico, 2009; Santos et al., 2012). Rocha et al. (2020) could as well not establish a unique proportionality between wood density and growth rate. The authors concluded, that beside a fundamental genetic effect on wood density, there is a strong interaction between genetics and the growth environment. They speculate, that variation in wood density may change the carbon concentration in the secondary xylem.

Studies conducted in the same research area as our study were not consistent with respect to the effects of spacing on wood density. Whereas Garcia et al. (1991) found for 10-year-old *Eucalyptus grandis* and *Eucalyptus saligna* trees decreasing average wood density with increasing spacing, Magalhães et al. (2020) observed on eucalypt clonal material (clones of hybrids of *Eucalyptus urophylla* x *Eucalyptus grandis*) at the age of 35 months higher average wood density in wider spacings. Malan and Hoon (1992) explain the higher average wood density they observed at South African *Eucalyptus grandis* trees growing at wider spacings with the phenomenon, that trees growing more freely begin to produce mature wood at an earlier age, reaching faster higher density levels.

Wimmer et al. (2002) analyzed the daily radial growth of 6-year-old *Eucalyptus nitens trees* using point dendrometers under different irrigation regimes. It was found that early in the growing season lower density wood was formed, and higher wood density later. The irrigated-droughted trees responded with decreasing wood density in response to water stress releases. This density decrease was accompanied by acceleration in daily increment. In another study on the effects of irrigation on wood density of 8-year-old *Eucalyptus globulus* trees Drew et al. (2011) found, that continuous irrigation led to the production of wood with significantly more homogenous density than trees experiencing large fluctuations in temporal water availability. They showed that trees which were not irrigated had the highest overall wood density. This agrees with Rocha et al. (2020) who found that maximum atmospheric vapor-pressure deficit and soil water deficit were the most significant variables to estimate the basic wood density of Eucalyptus clones of different species. Interestingly Halder et al. (2021) observed for *Eucalyptus camaldulensis* trees growing in agroforestry systems in Bangladesh significantly higher average wood density on a dry site, i.e. a site with low precipitation (age: 20 years), compared to a high precipitation site (age: 13 years). The authors hypothesized, that lower wood density at the high precipitation site is due to higher volumetric growth rates for a given amount of carbon assimilation. They noticed that low density woody tissue has higher hydraulic conductivity and thus capacity to supply more water to a greater photosynthetic capacity in leaves than trees with high wood density (Chave et al., 2009).

Although in our study the clone COP 1404 is the genetic material with the highest average wood density, it also presented the lowest growth rates, which suggests that the slower-growing trees tend to have a higher wood density, in this case, regardless of the spacing. The growth rate is strongly dependent on carbon gain, which in turn depends on the rate of photosynthetic CO_2 assimilation (Holland et al., 2019). Rodrigues et al. (2021), evaluating the production and carbon allocation in the same area of this study observed the clonal ranking for annual leaf production as AEC 144 > AEC 224 > COP 1404. This may be associated with a lower net photosynthetic rate for COP 1404 that consequently contributed to a lower growth rate in comparison with the other clones. Momentel (2016), evaluating the growth of the clones AEC 144, AEC 224, and COP 1404, observed that COP 1404 showed a reduction in leaf area as an avoidance mechanism to water stress. Several studies with other species reported similar effects caused by water stress (Silva et al., 2004, Otieno et al., 2005, Guerfel et al., 2009, Waghorn et al., 2015). Taiz and Zeiger (2013) report that the reduction in leaf area leads to lower evapotranspiration rates, allowing the use of limited water supply in the soil for a longer period. However, once that growth and productivity are directly related to the total leaf area, a decrease in the values of the leaf area can reflect in lower tree growth rates (Weraduwage et al., 2015).

4.2. *Assessment of the alignment and annotation methods*

When tree growth is governed by strong seasonal constraints, detection of annual/seasonal growth patterns is possible based on optical or densitometric measures (Salzer et al., 2009; Drew et al., 2012; Balzano et al., 2020). Studies around the world provide increasing evidence for an association between intra-annual wood density and climate events, especially to changes in temperature and rainfall (Roque and Tomazello Filho, 2007; van der Maaten et al., 2012; González-Cásares et al., 2019; Mayer et al., 2020).

Although annual tree-rings can provide the opportunity to study the impacts of climatic factors on its growth (Brookhouse et al., 2008), many Eucalypts in tropical zones do not form distinct growth rings. Thus, a new semi-automated protocol was suggested within this work, to enable temporal annotation not only on a seasonal but high-resolution level.

In its current setup, the spatial alignment of individual density measurement series is based on a manual identification and annotation of radial variations in visible wood anatomical properties. Such data preparation is only applicable to low sample sizes. To upscale the workflow, automated registration methods, e.g. based on (sub)image alignment (Chakraborty et al., 2016), have to be developed.

Given our temporal annotation, we observe a decrease in spatial width with increasing age and dimension of the tree. Due to the equidistant uniform density sampling along radial axes, this results in a strong disparity of the density data resolution per year. While this is corrected in the end via respective smoothing functions to provide a uniform data curve, higher noise in high resolution data poses another difficulty for spatial alignment of density measurement series with unknown annual boundaries.

4.3. Validation of temporal annotation via correlation with climate data

Wood density is considered a heritable trait, with a strong phylogenetic signal, and is strongly affected by climatic variation (Oberhuber et al., 2014; Nabais et al., 2018). We found that precipitation and the climatic water balance had negative effects on wood density at the intra-annual time scale, being in general, the precipitation the variable with the strongest correlation (Fig. 8). This means that in a period with less rain, the trees responded with an increase in the wood density. Wimmer et al. (2002) made similar observations and used dendrometer measurements to rescale wood density on a time axis.

According to Zahner (1963), drought periods is conducive to the formation of high-density wood. Lower rainfall rates contribute to the formation of fibrous structures with thicker walls, smaller vessels and a lower vessel frequency (Malan, 1995; Fichtler and Worbes, 2012), which favor an increase in the gravimetric wood density. Sette et al. (2016), evaluating the relationship between climate variables, trunk growth rate, and wood density of *Eucalyptus grandis* W. Mill ex Maiden trees observed a high sensitivity of wood density to precipitation, showing that a higher/lower precipitation level implies a lower/higher average density of the wood of *Eucalyptus* trees.

For all clones and both spacings, a significant negative correlation ($p < 0,1$) between precipitation and wood density profiles was observed. Drew et al. (2009), using the re-scale method to evaluate the wood properties in *E. globulus* trees, reported that changes in environmental conditions, especially the increase in the water availability in the soil, affected negatively the wood density. According to Schonau and Coetzee (1989), as trees grow, their crowns and roots quickly influence the space of the individuals around, resulting in an intense competition for factors of growth, such as water, light, and nutrients. Therefore, wider spacings provide larger productive capacity for the trees due to less competition for resources (Rodrigues et al., 2021). An increase in wood density has been associated with decreased soil water supply in *Eucalyptus nitens* (Wimmer et al., 2002). Nyakuengama et al. (2002), evaluating the growth and wood proprieties responses to later-age fertilizer application in *Pinus radiata*, found that soil-water-storage affected the wood density of the trees, being higher in *Pinus radiata* grown on well-drained, sandy soils than on clay soils with higher water storing capacity (Costa et al., 2013).

Verification of the spatial alignment and temporal annotation could be supported by the use of high resolution dendrometer data and by xylogenesis studies based, e.g. on the analysis of microcores.

Climatic and weather conditions are the principal factors that determine the choice of genetic material for forest plantations, since the weather conditions influence the growth rates and wood properties of Eucalyptus species (Gonçalves et al., 2004; Binkley et al., 2017; Elli et al., 2020). In this study, Clone AEC 144 showed the strongest effect of precipitation on wood density (Fig. 8) and the highest loading on PC1 (Fig. 7).

5. Conclusions

Three different *Eucalyptus urophylla* clones grown in two different spacing regimes at an experimental site in humid subtropical climate in Brazil have been analyzed to test effects of clone identity, spacing, cambial age and hydroclimatic conditions on high-resolution intra-annual wood density profiles. As distinct tree-ring boundaries were not visible on the stem cross-sectional surfaces, an alternative method for synchronizing the density profiles within and between the sample trees had to be found. We defined this registration problem as the search for a set of data processing steps to generate intra- and inter-tree synchronized density profiles that possess high amplitude and low phase variation. To achieve this, we developed a protocol and workflow of how such high-resolution density profiles can first be spatially aligned and second temporally annotated, to enable correlation analyses among and between trees and with time series of environmental stimuli.

We found that the average wood density was significantly different between clones, but not between the spacings. Intra-annual wood density increased with increasing cambial age and with decreasing daily growth rate. Multivariate analysis of the temporally aligned sequences revealed that the variability in the density profiles is dominated by a synchronous, highly significant common signal. We identified water availability as the main driver of variation in stem growth rate at the site.

The workflow of synchronizing high-resolution intra-annual density profiles is described and presented as a flowchart, consisting of four basic steps (Fig. 2). In the presented formulation the data processing functions and processes in each of the four steps are directed towards the analysis of high-resolution intra-annual density profiles. However, by modifying these data processing functions and processes the basic workflow can easily be adjusted to the analysis of other intra-annual tree-ring features like anatomical xylem cell traits or isotopic signals in the wood. Hence, the developed workflow has a large potential to be used as a guideline for the synchronization of intra-annual tree-ring traits, especially when distinct tree-ring boundaries are missing, as it is often the case under tropical climatic conditions. The workflow supports the development of spatially aligned and temporally annotated chronologies under non-annual or not strictly annual growth rhythms.

Declaration of Competing Interest

The authors declare that they have no known competing financial interests or personal relationships that could have appeared to influence the work reported in this paper.

Acknowledgments

GGR received financial support from the Coordenação de Aperfeiçoamento de Pessoal de Nível Superior - Brasil (CAPES) - Finance Code 001.

Appendix A. Supporting information

Supplementary data associated with this article can be found in the online version at doi:10.1016/j.dendro.2022.125978.

References

Allen, K., Drew, D., Downes, G., Evans, R., Baker, P., Grose, M., 2012. Ring width, climate and wood density relationships in two long-lived Tasmanian tree species. Dendrochronologia 30, 167–177.

Allen, R.G., Pereira, L.S., Raes, D., Smith, M., 1998. Crop Evapotranspiration: Guidelines for Computing Crop Water Requirements. FAO, Rome, p. 300 (Irrigation and Drainage Paper).

Argent, R.M., McMahon, T.A., Bowler, J.M., Finlayson, B.L., 2004. The dendroecological potential of Eucalyptus camaldulensis Dehnhardt (River Red Gum) from the Barmah Forest, Victoria, Australia. Aust. Geogr. Stud. 42, 89–102.

Balzano, A., Battipaglia, G., Cherubini, P., De Micco, V., 2020. Xylem plasticity in pinus pinaster and quercus ilex growing at sites with different water availability in the mediterranean region: relations between intra-annual density fluctuations and environmental conditions. Forests 11, 379.

Battie-Laclau, P., Laclau, J.P., Domec, J.C., Christina, M., Bouillet, J.P., Piccolo, M.C., Gonçalves, J.L.M., 2014. Effects of potassium and sodium supply on drought-adaptive mechanisms in Eucalyptus grandis plantations. N. Phytol. 203, 401–413.

Bender, B., Mann, M., Backofen, R., Spiecker, H., 2012. Microstructure alignment of wood density profiles: an approach to equalize radial differences in growth rate. Trees - Struct. Funct. 26, 1267–1274.

Binkley, D., Campoe, O.C., Alvares, C., Carneiro, R.L., Cegatta, Í., Stape, J.L., 2017. The interactions of climate, spacing and genetics on clonal Eucalyptus plantations across Brazil and Uruguay. For. Ecol. Manag. 405, 271–283.

Briffa, K.R., Osborn, T.J., Schweingruber, F.H., Jones, P.D., Shiyatov, S.G., Vagano, E.A., 2002. Tree-ring width and density data around the Northern Hemisphere: part 1, local and regional climate signals. Holocene 12, 737–757.

Brookhouse, M., 2006. Eucalypt dendrochronology: past, present and potential. Aust. J. Bot. 54, 435–449.

Brookhouse, M., Lindesay, J., Brack, C., 2008. The potential of tree rings in eucalyptus pauciflora for climatological and hydrological reconstruction. Geogr. Surv. 46, 421–434.

Brown, A.G., Nambiar, E.K.S., Cossalter, C., 1997. Plantations for the tropics – Their role, extent and nature. Monograph 43. In: Nambiar, E.K.S., Brown, A.G. (Eds.), Management of soil, water and nutrients in tropical plantation forests. Australian Centre for International Agricultural Research (ACIAR), Canberra, pp. 1–23.

Chakraborty, S., Patra, P.K., Maji, P., Ashour, A.S., 2016. Image Registration Techniques and Frameworks: A Review. In: Proc. Appl. Video Process. Surveill. Monitor. Syst, 2017. IGI Global, pp. 102–114.

Chave, J., Coomes, D., Jansen, S., Lewis, S.L., Swenson, N.G., Zanne, A.E., 2009. Towards a worldwide wood economics spectrum. Ecol. Lett. 12, 351–366.

Christina, M., Laclau, J.P., Gonçalves, J.L.M., Jourdan, C., Nouvellon, Y., Bouillet, J.-P., 2011. Almost symmetrical vertical growth rates above and below ground in one of the world's most productive forests. Ecosphere 2, 1–10.

Cosgrove, D.J., 2016. Biophysical control of plant cell growth. Ann. Rev. Plant Biol. 37, 377–405.

Costa, A., Albuquerque, J.A., Costa, A., Pértile, P., Silva, F.R., 2013. Water retention and availability in soils of the State of Santa Catarina-Brazil: effect of textural classes, soil classes and lithology. Rev. Bras. Cienc. Solo 37, 1535–1548.

D'Arrigo, R.D., Jacoby, G.C., Free, R.M., 1992. Tree-ring width and maximum latewood density at the North American tree line: parameters of climatic change. Can. J. Res 22, 1290–1296.

Dawdy, D.R., Matalas, N.C., 1964. Statistical and Probability Analysis of Hydrologic Data, Part III: Analysis of Variance, Covariance and Time Series. Handbook of applied hydrology, a compendium of water-resources technology. McGraw-Hill Book Company, New York, pp. 8.68–8.90.

Drew, D., Downes, G.M., O'Grady, A.P., Read, J., Worledge, D., 2009. High resolution temporal variation in wood properties in irrigated and non-irrigated Eucalyptus globulus. Ann. Sci. 66, 406-406.

Drew, D., Downes, G.M., Evans, R., 2011. Short-term growth responses and associated wood density fluctuations in variously irrigated Eucalyptus globulus. Trees 25, 153–161.

Drew, D., Allen, K., Downes, K., Evans, R., Battaglia, M., Baker, P., 2012. Wood properties in a long-lived conifer reveal strong climate signals where ring-width series do not. Tree Physiol. 33, 37–47.

Eilers, P.H.C., 2004. Parametric time warping. Anal. Chem. 76, 404–411.

Elli, E.F., Sentelhas, P.C., Huth, N., Carneiro, R.L., Alvares, C.A., 2020. Gauging the effects of climate variability on Eucalyptus plantations productivity across Brazil: A process-based modelling approach. Ecol. Indic. 114, 106325.

FAO, 2014. The State of the World's Forest Genetic Resources. Rome 304.

Fichtler, E., Worbes, M., 2012. Wood anatomical variables in tropical trees and their relation to site conditions and individual tree morphology. IAWA J. 33, 119–140.

Franceschini, T., Longuetaud, F., Bontemps, J.-D., Bouriaud, V., Caritey, B.-D., Leban, J.-M., 2013. Effect of ring width, cambial age, and climatic variables on the within-ring wood density profile of Norway spruce *Picea abies* (L.) Karst. Trees 27, 913–925.

Frederico, P.G.U., 2009. Efeito da região e na madeira de eucalipto nas propriedades do carvão vegetal. (in Portuguese, with English abstract) (Dissertation). Universidade Federal de Viçosa.

Garcia, C.H., Corradine, L., Alvarenga, S.F., 1991. Comportamento florestal do *Eucalyptus grandis* e *Eucalyptus saligna* em diferentes espaçamentos. (in Portuguese, with English abstract). IPEF 179, 1–8.

George, J.P., Grabner, M., Campelo, F., Karanitsch-Ackerl, S., Mayer, K., Klumpp, R.T., Schüler, S., 2019. Intra-specific variation in growth and wood density traits under water-limited conditions. Long-term-, short-term-, and sudden responses of four conifer tree species. Sci. Total Environ. 660, 631–643.

Gonçalves, J.L.M., Stape, J.L., Laclau, J.P., Smethurst, P., Gava, J.L., 2004. Silvicultural effects on the production and wood quality of eucalypt plantations. For. Ecol. Manag. 193, 45–61.

González-Cásares, M., Pompa-García, M., Venegas-González, A., 2019. Climate signals from intra-annual wood density fluctuations in Abies durangensis. IAWA J. 40, 276–287.

Guerfel, M., Baccouri, O., Boujnah, D., Chaïbi, W., Zarrouk, M., 2009. Impacts of water stress on gas exchange, water relations, chlorophyll content and leaf structure in the two main Tunisian olive (*Olea europaea* L.) cultivars. Sci. Hortic. 119, 257–263.

Halder, N.K., Chowdhury, M.Q., Fuentes, D., Possell, M., Merchant, A., 2021. Intra-specific patterns of δ13C, growth and wood density variation at sites of contrasting precipitation with implications for modelling carbon sequestration of tropical tree species. Agrofor. Syst. 95, 1429–1443.

Holland, B., Monk, N., Clayton, R., Osborne, C., 2019. A theoretical analysis of how plant growth is limited by carbon allocation strategies and respiration. Silico Plants 1, 1–18.

IAWA, 1964. Multilingual glossary of terms used in wood anatomy. English version. Mitt. der Schweiz. Anst. für Das. Forstl. Vers. 40, 27–46.

IBGE, 1972. Climatologia da região sudeste do Brasil introdução à climatologia dinâmica. (in Portuguese, with English abstract). Rev. Bras. Geog 34, 3–191.

Koprowski, M., Duncker, P., 2012. Tree ring width and wood density as the indicators of climatic factors and insect outbreaks affecting spruce growth. Ecol. Indic. 23, 332–337.

Laclau, J.-P., Ranger, J., Gonçalves, J.-L.M., Maquère, V., Krusche, A.V., M'Bou, A.T., Nouvellon, Y., Saint-André, L., Bouillet, J.P., Piccolo, M.C., Deleporte, P., 2010. Biogeochemical cycles of nutrients in tropical Eucalyptus plantations. Main features shown by 10 years of monitoring in Congo and Brazil. For. Ecol. Manag. 259, 1771–1785.

Magalhães, L.G.S., Lima, A.P.L., Lima, S.F., Seratto, D.N., Martins, S.M., 2020. Densidade básica da madeira de clones de eucalipto em diferentes espaçamentos. (in Portuguese, with English abstract). Braz. J. Dev. 6, 19435–19445.

Malan, F.S., Hoon, M., 1992. Effect of initial spacing and thinning on some wood properties of *Eucalyptus grandis*. South Afr. J. 163, 13–20.

Malan, F.S., 1995. Eucalyptus improvement for lumber production. Semin. Int. De. Util. da Madeir-.-. De. Eucalyptus Para. Serraria, São Paulo, Bras. IPEF/IPT/IUFRO/LCF/ESALQ/ USP 1–19.

Mann, M., Kahle, H.P., Beck, M., Bender, B.J., Spiecker, H., Backofen, R., 2018. MICA: Multiple interval-based curve alignment. SoftwareX 7, 53–58.

Mayer, K., Grabner, M., Rosner, S., Felhofer, M., Gierlinger, N., 2020. A synoptic view on intra-annual density fluctuations in Abies alba. Dendrochronologia 64, 125781.

Melo, L.E.L., Silva, J.R.M., Napoli, A., Lima, J.T., Trugilho, P.F., Nascimento, D.F.R., 2016. Influence of genetic material and radial position on the anatomical structure and basic density of wood from *Eucalyptus spp.* and *Corymbia citriodora.* Sci 111, 611–621.

Momentel, L.T. 2016. Crescimento e eficiência no uso da água por clones de eucalipto sob doses de potássio. (in Portuguese, with English abstract). Dissertation. Escola Superior de Agricultura "Luiz de Queiroz", Universidade de São Paulo.

Myburg, A., Grattapaglia, D., Tuskan, G.G., Schmutz, J., 2014. The genome of *Eucalyptus grandis.* Nature 510, 356–362.

Nabais, C., Hansen, J.K., David-Schwartz, R., Klisz, M., López, R., Rozenberg, P., 2018. The effect of climate on wood density: What provenance trials tell us? For. Ecol. Manag. 408, 148–156.

Nyakuengama, J.G., Downes, G.M., Ng, J., 2002. Growth and wood density responses to later-age fertilizer application in Pinus radiata. IAWA J. 23, 431–448.

Oberhuber, W., Gruber, A., Kofler, W., Swidrak, I., 2014. Radial stem growth in response to microclimate and soil moisture in a drought-prone mixed coniferous forest at an inner Alpine site. Eur. J. Res 133, 467–479.

Oliveira, B.R.U., Latorraca, J.V.F., Tomazello Filho, M., Garcia, R.A., Carvalho, A.M., 2011. Dendroclimatology correlations of eucalyptus grandis hill ex maiden of Rio Claro, RJ State - Brazil. Ciênc Flore 21, 499–508.

Otieno, D.O., Schmidt, M.W.T., Adiku, S., Tenhunen, J., 2005. Physiological and morphological responses to water stress in two Acacia species from contrasting habitats. Tree Physiol. 25, 361–371.

Polge, H., 1970. The use of X-ray densitometric methods in dendrochronology. Tree Ring Bull. 30, 1–10.

Rocha, S.M.G., Vidaurre, G.B., Pezzopane, J.E.M., Almeida, M.N.F., Carneiro, R.L., Campoe, O.C., et al., 2020. Influence of climatic variations on production, biomass and density of wood in eucalyptus clones of different species. For. Ecol. Manag. 473, 118290.

Rodrigues, G.G., Silva, L.D., Nouvellon, Y., 2021. Production and carbon allocation in clonal Eucalyptus plantations under different planting spacings. For. Ecol. Manag. 493, 119249.

Roque, R.M., Tomazello Filho, M., 2007. Relationships between anatomical features and intra-ring wood density profiles in Gmelina arborea applying X-ray densitometry. Cerne 13, 384–392.

Salzer, M.W., Hughes, M.K., Bunn, A.G., Kipfmueller, K.F., 2009. Recent unprecedented tree-ring growth in bristlecone pine at the highest elevations and possible causes. PNAS 106, 20348–20353.

Santos, L.C., Carvalho, A.M.M.L., Pereira, B.L.C., Oliveira, A.C., Carneiro, A.C.O., Trugilho, P.F., 2012. Propriedades da madeira e estimativas de massa, carbono e energia de clones de Eucalyptus plantados em diferentes locais. (in Portuguese, with abstract in English). Rev. Árvore 36, 971–980.

Schinker, M., Hansen, N., Spiecker, H., 2003. High-frequency densitometry – a new method for the rapid evaluation of wood density variations. IAWA J. 24, 231–239.

Schönau, A.P.G., Coetzee, J., 1989. Initial spacing, stand density and thinning in eucalypt plantations. For. Ecol. Manag. 29, 245–266.

Schweingruber, F.H., 1982. Measurement of densitometric properties of wood. In: Hughes, M.K., Kelly, P.M., Pilcher, J.R., Lamarche, J.V.C. (Eds.), Climate From Tree Rings, pp. 107–114.

Sette Jr., C.R., Tomazello Filho, M., Lousada, J.D., Lopes, D., Laclau, J.P., 2016. Relationship between climate variables, trunk growth rate and wood density of Eucalyptus grandis W. Mill ex Maiden trees. Rev. Árvore 40, 337–346.

Silva, F.C., Shvaleva, A., Maroco, J.P., Almeida, M.H., Chaves, M.M., Pereira, J.S., 2004. Responses to water stress in two Eucalyptus globulus clones differing in drought tolerance. Tree Physiol. 24, 1165–1172.

Spiecker, H., Schinker, M.G., Hansen, J., Park, Y.-I., Döll, W., 2000. Cell structure in tree rings: Novel methods for preparation and image analysis of large cross sections. IAWA J. 21, 361–373.

Stahle, D.W., 1999. Useful strategies for the development of tropical tree-ring chronologies. IAWA J. 20, 249–253.

Taiz, L., Zeiger, E., 2013. Fisiologia vegetal. [Plant Physiology], Fourth ed. Artmed, Porto Alegre, p. 848.

Tomazello Filho, M., Lisi, C.S., Hansen, N., Cury, G., 2004. Anatomical features of increment zones in different tree species in the State of São Paulo, Brazil. Sci 66, 46–55.

van der Maaten, E., van der Maaten-Theunissen, M., Spiecker, H., 2012. Temporally resolved intra-annual wood density variations in European beech (*Fagus sylvatica* L.) as affected by climate and aspect. Ann. Res 55, 113–124.

Waghorn, M.J., Whitehead, D., Watt, M.S., Harrington, J.J., 2015. Growth, biomass, leaf area and water-use efficiency of juvenile Pinus radiata in response to water deficits. N. Z. J. Sci. 45, 3.

Wassenberg, M., Montwé, D., Kahle, H.P., Spiecker, H., 2014. Exploring High-frequency densitometry calibration functions for different tree species. Dendrochronologia 32, 273–281.

Weraduwage, S.M., Chen, J., Anozie, F.C., Morales, A., Weise, S.E., Sharkey, T.D., 2015. The relationship between leaf area growth and biomass accumulation in Arabidopsis thaliana. Front Plant Sci. 6, 167.

Wils, T.H.G., Robertson, I., Eshetu, Z., Sass-Klaassen, U.G.W., Koprowski, M., 2009. Periodicity of growth rings in Juniperus procera from Ethiopia inferred from crossdating and radiocarbon dating. Dendrochronologia 27, 45–58.

Wimmer, R., Downes, G.M., Evans, R., 2002. High-resolution analysis of radial growth and wood density in Eucalyptus nitens, grown under different irrigation regimes. Ann. Sci. 59, 519–524.

Worbes, M., 2002. One hundred years of tree-ring research in the tropics - a brief history and an outlook to future challenges. Dendrochronologia 20, 217–231.

Zahner, R., 1963. Internal moisture stress and wood formation in conifers. Prod. J. 13, 240–247.